Role of Mixing Parameters in the Preparation of Poly(ethylene vinyl acetate) Nanocomposites by Melt Blending

Mangala Tillekeratne, Margaret Jollands, Ferenc Cser, Sati N. Bhattacharya

Rheology and Materials Processing Centre, School of Civil and Chemical Engineering, Royal Melbourne Institute of Technology (RMIT) University, Australia

Received 27 July 2004; accepted 5 June 2005
DOI 10.1002/app.22755
Published online 9 February 2006 in Wiley InterScience (www.interscience.wiley.com).

ABSTRACT: Polymer/layered-silicate nanocomposites have gathered momentum as cost-effective and versatile materials since the middle of the 20th century. Many publications discuss the chemistry of organomodification and properties of nanocomposites, but relatively few deal with the significance of processing conditions. This article takes into account three mixing parameters and discusses the contribution of each toward nanocomposite formation. Organomodified natural sodium-type bentonite clay was used in this study. The nanocomposites formed were characterized by X-ray diffraction and mechanical property tests. Response surface regression was used to optimize the tensile modulus. The analysis shows that nanocomposite formation is promoted by a diffusion mechanism and that the interactions of parameters are as important as individual parameters. © 2006 Wiley Periodicals, Inc. J Appl Polym Sci 100: 2652–2658, 2006

Key words: copolymerization; processing; nanocomposites; WAXS

INTRODUCTION

Nanocomposites were first reported in the patent literature[1] as early as 1950. Because of the work published by Toyota Motor Co.,[2–5] a great deal of attention has since been focused on polymer/layered-silicate nanocomposites. Toyota's work was mainly based on polyamide nanocomposites, and the method used to prepare them was in situ polymerization, in which clay is swollen (intercalated) in a liquid monomer and then polymerization follows within the interlayer spacing or galleries of clay platelets. This technique has been used in the preparation of nanocomposites from many host polymers and has proved successful in making nanocomposites from both thermoplastic and thermoset resins with superior properties. Solution intercalation was also used in the early days.[6]

Unfortunately, for some technologically important polymers, these traditional methods are limited because of the nonavailability of a suitable monomer or a compatible solvent. Therefore, making nanocomposites via the melt blending of the polymer and the organoclay has been explored. This approach also reduces the volumes of chemical reagents that must be handled and is more compatible with current processing techniques. However, the processing conditions necessary to achieve the desired level of nanodispersion are less well documented.

Several factors contribute to nanocomposite formation, such as the polarity of the polymer, organic modification, and processing conditions. If the host polymer and clay are highly compatible, polymer chains can diffuse into the galleries, forming an intercalated nanocomposite even under static conditions.[7,8] However, for some polymer/clay systems, the processing conditions may play a vital role in successfully delaminating the clay platelets. The effects of processing conditions on the delamination of clay platelets in polyamide were reported by Dennis et al.[9] In that study, the shear intensity was changed qualitatively through changes in the screw configuration. It was concluded that a screw configuration that gave medium shear was able to produce exfoliated nanocomposites. The structure and properties of ethylene vinyl acetate and organoclay (Closite 15A) nanocomposites formed under different processing conditions were reported by Mantia et al.[10] In this study, only the temperature and rotor speed were considered at two levels (temperature = 110 and 160°C, rotor speed = 150 and 250 rpm) However, the interaction of the parameters was not considered. Small differences were observed as a function of the processing conditions.

The processing conditions are affected not only by individual parameters such as the barrel temperature,

Correspondence to: S. N. Bhattacharya (s2114325@student.rmit.edu.au).

mixing time, and rotor speed but also by their interactions. For example, it is well known that the melting temperature during mixing is affected by both the barrel temperature and screw speed. Therefore, it is necessary to understand the effects of these parameters on the intercalation and exfoliation processes to optimize the mixing conditions. This study was aimed at assessing quantitatively the significance of the mixing parameters, namely, the barrel temperature, mixing time, and rotor speed, and their interactions.

The nanocomposites of interest here are made of poly(ethylene vinyl acetate) with an acetate concentration of 9% (EVA9) and organoclay. The organoclay is based on a sodium-type bentonite, which has a layered structure with a high aspect ratio and a high surface area, typically 750 m^2/g. The aspect ratio depends on the source of clay. A clay particle 8 μm in diameter contains about 3000 clay platelets.[11] The thickness of each platelet is around 1 nm. The challenge in blending is to break these particles into individual platelets and disperse them homogeneously in the polymer matrix.

To overcome this challenge, it is useful to know how effective the mixing parameters are in producing intercalated and exfoliated nanocomposites. Mechanical properties are sensitive to the degree of intercalation and exfoliation. It is well known that exfoliation produces better properties.

EXPERIMENTAL

Materials

EVA9 with a melt flow index of 3/g min was provided by Cryovac Australia Pty., Ltd. Sodium-type bentonite was supplied by Unimin Australia, Ltd., and was used without further purification. It was organomodified with cetyl dimethylethyl ammonium bromide in RMIT's laboratories with a cation-exchange reaction. All compounds were prepared with 5 wt % organoclay (cetyl clay) unless differently stated. The average particle size of the cetyl clay was 33 μm.

Experimental design

The nanocomposites in this study were made in a Haake Rheocord 90 internal mixer (Instron Corporation, Norwood, MA), which allowed good control over the test parameters. Three factors, namely, the temperature, mixing time, and rotor speed, were selected as the independent variables in the experimental design. The set temperature of the mixer was used because controlling the melting temperature of the mix was not possible in the Haake Rheocord. The melting temperature depended on viscous heating generated by the rotors as well as the chamber temperature. Each factor was considered at two levels, and the chosen design was a full factorial with eight runs. Factor levels were chosen arbitrarily on the basis of the literature and previous knowledge and experience. Three runs at the center point were carried out to estimate the experimental error and to check for quadratic effects (Table I).

TABLE I
Experimental Design for the Preparation of Cetyl Nanocomposites

Temperature (°C)	Mixing time (min)	Rotor speed (rpm)
	10	
90	20	30
	10	
100	20	110

Center point: temperature = 95°C; mixing time = 15 min; rotor speed = 170.

X-ray diffraction

Wide-angle X-ray scattering (WAXS) patterns were obtained with a Philips X-ray diffractometer with Ni-filtered Cu Kα radiation with a wavelength of 1.54 Å at room temperature. WAXS was recorded in transmission mode with a rotating sample holder from 2θ = 1.2–30° in 0.05 steps. The slit width was 0.6 mm. Background diffraction was recorded and removed from the sample diffraction data.

Environmental scanning electron microscopy (ESEM)

The morphology of the nanocomposites was examined with an FEI Quanta200 environmental scanning electron microscope (Instron Corp.). The acceleration voltage was 20 kV. The secondary images were collected, and the resolution of the image was 3 nm.

Mechanical properties

The Young's modulus, tensile strength, and elongation at break were determined with an Instron model 4467 tester (Instron Corp.) in accordance with standard test method ASTM D 638. A grip separation speed of 100 mm/min was used. The samples were conditioned at 25 ± 1°C and 50% relative humidity for 48 h before testing. The results were analyzed with the Minitab 13.2 statistical package (Minitab, Inc., State College, PA).

RESULTS AND DISCUSSION

The compression-molded plaques were visually inspected and appeared to be homogeneous and appreciably transparent.

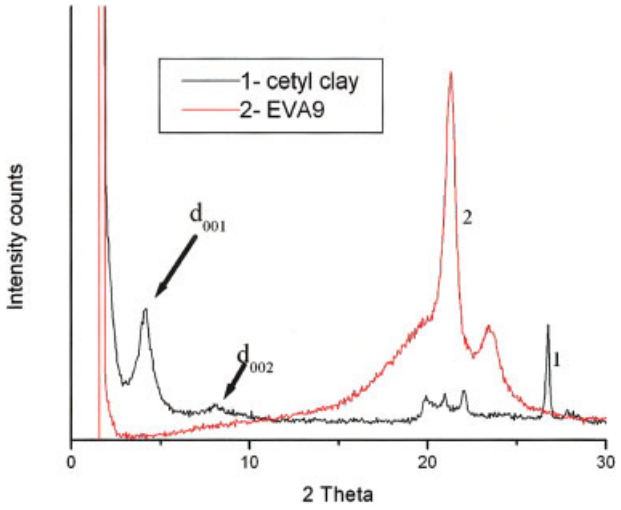

Figure 1 X-ray diffraction patterns of cetyl clay and EVA9. [Color figure can be viewed in the online issue, which is available at www.interscience.wiley.com.]

The WAXS patterns obtained for cetyl clay and EVA9 are shown in Figure 1. Cetyl clay shows an intense peak (d_{001}) at $2\theta = 4.2°$ (21.0 Å) and a second peak (d_{002}) at $2\theta = 8°$ (10.8 Å). EVA9 shows no diffraction peaks in this region. A typical diffraction pattern obtained for a nanocomposite is shown in Figure 2, and the peak positions are given in Table II. All the curves show a stronger scattering intensity near the primary beam than the EVA9 WAXS pattern. The strengthening of the scattering near the primary beam could be due to the superimposition of d_{001} with the primary beam. They also show a prominent peak around $2\theta = 4.45°$ (19.8 Å). This corresponds to a shorter interlayer distance than that of pure cetyl clay. A trace of a peak can also be observed around $2\theta = 2°$ (44 Å). If this trace peak corresponds to d_{001}, then the peak appearing around $2\theta = 4.45°$ (19.8 Å) corresponds to d_{002}. This arrangement represents an intercalated system with an interlayer distance of about 40 Å. If the peak at $2\theta = 4.45°$ corresponds to d_{001}, the strengthening of the primary beam and the loss of intensity of the peak at $2\theta = 4.45°$ indicate the exfoliation of some of the clay platelets. This leads to particle scattering and results in stronger particle scattering near the primary beam. A similar movement of a peak to higher angles (lower interlayer distance) was observed by Zanetti et al.[12] They attributed this movement to higher angles to either impurities present in the system or partial decomposition of the organoclay followed by the collapse of the interlayer. However, they did not rule out the presence of a peak corresponding to a higher interlayer distance being outside the detectable range of the instrument used in their study. They concluded that the system was still an intercalated system despite the absence of recognizable d_{001} and d_{002} peaks. Similar observations were reported by Jeon et al.[13] Mantia et al.[10] also reported an intercalated structure with an interlayer distance of about 44 Å for Closite 15A and film-grade poly(ethylene vinyl acetate). Other data reported later in this article support the interpretation that $2\theta = 2°$ and $2\theta = 4.45°$ are d_{001} and d_{002} peaks.

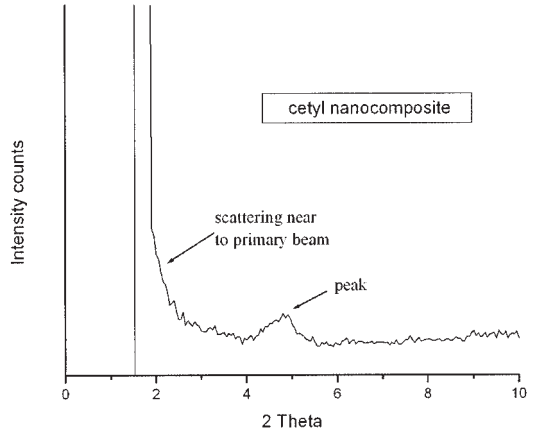

Figure 2 Typical WAXS pattern of an EVA9/cetyl nanocomposite.

TABLE II
Peak Positions of Nanocomposites

	2θ (°)	
Temperature/time/rpm	Peak 1	Peak 2
100/10/110	~2.05	4.55
90/20/30	~2.0	4.5
100/20/30	~2.1	4.55
100/20/110	~2.15	4.35
95/15/70	~2.05	4.25
90/20/110	~2.0	4.25
90/10/30	~2.15	4.3
100/10/30	~2.2	4.2

A typical image obtained for EVA9/cetyl nanocomposites with ESEM is shown in Figure 3. This shows particles with a high aspect ratio and a thickness in the range of ~80–700 nm. This suggests an intercalated structure, supporting our WAXS data. The arrangement of particles also shows some orientation, which may be the result of flow during compression molding.

The modulus was measured for these composites because the modulus is considered to be an indicator of the extent of intercalation/exfoliation.[14] The tensile properties of the nanocomposites are given in Figures 4–6. The values are the average of a minimum of four samples. The standard deviation is 8% for the tensile modulus and 5% for the tensile strength and elongation.

All the nanocomposites showed an increase in the modulus in comparison with EVA9 (Fig. 4). The increase varied from 8 to 34% and was 23% on average. Alexandre et al.[15] reported a 100% increase in the

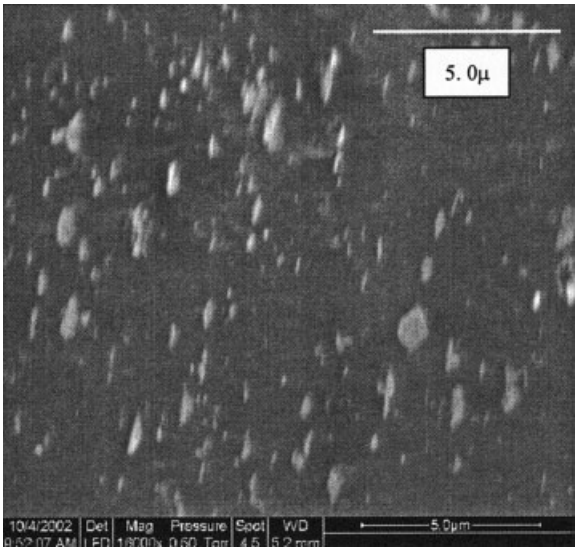

Figure 3 Typical ESEM picture of a poly(ethylene vinyl acetate)/cetyl nanocomposite.

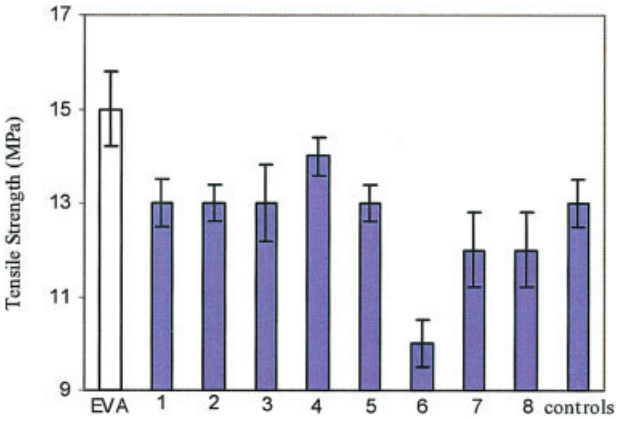

Figure 5 Tensile strength of nanocomposites made under different processing conditions (sample code: temperature/mixing time/rpm): (1) 100/10/110, (2) 90/20/30, (3) 100/20/30, (4) 100/20/110, (5) 90/20/110, (6) 90/10/30, (7) 90/10/110, and (8) 100/10/30. The control was 95/15/70. [Color figure can be viewed in the online issue, which is available at www.interscience.wiley.com.]

modulus for semi-intercalated, semiexfoliated poly(ethylene vinyl acetate) (10.8% vinyl acetate) nanocomposites obtained with a different organomodification. In a separate study, Alexandre et al.[16] reported a 73% increase in the Young's modulus for intercalated poly(ethylene vinyl acetate) (27% vinyl acetate) nanocomposites with dimethyl dioctadecyl modified montmorillonite. It was also shown by Dennis et al.[9] that the degree of delamination (exfoliation) and dispersion (tendency to break up agglomerates) is affected by the clay treatment in polyamide nanocomposites. The lower increase in modulus observed here may therefore be due to several reasons. In general, if the structure is intercalated, the modulus is expected to be lower than if the structure were exfoliated. The clay/polymer interface may be weaker as the clay has organic chains residing on the surface, unlike the other studies, influencing the stress-transfer ability of the polymer. Two clays from two different sources are also likely to have different aspect ratios. The Young's modulus increases with the aspect ratio in composites.[17]

A decrease in the tensile strength and elongation at break was observed in all the nanocomposites in comparison with EVA9 (Figs. 5 and 6); similar trends in data were reported by Alexander et al.[15] and Jeon et

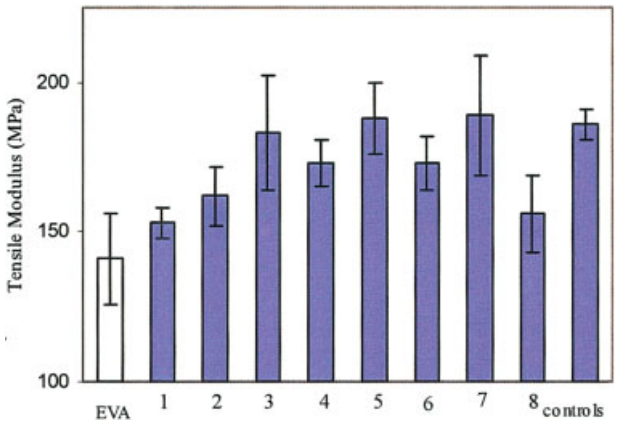

Figure 4 Tensile moduli of nanocomposites made under different processing conditions (sample code: temperature/mixing time/rpm): (1) 100/10/110, (2) 90/20/30, (3) 100/20/30, (4) 100/20/110, (5) 90/20/110, (6) 90/10/30, (7) 90/10/110, and (8) 100/10/30. The control was 95/15/70. [Color figure can be viewed in the online issue, which is available at www.interscience.wiley.com.]

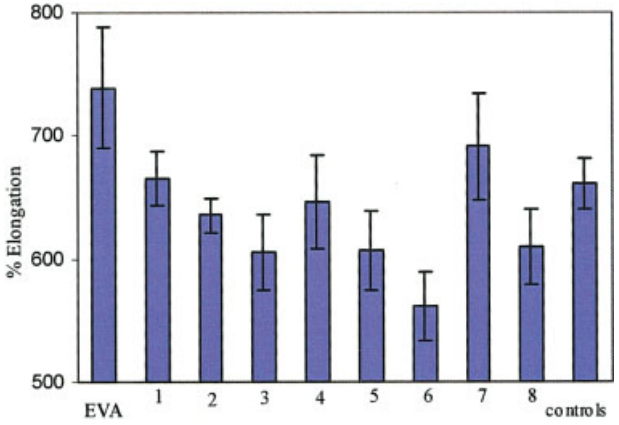

Figure 6 Elongation at break of nanocomposites made under different processing conditions (sample code: temperature/mixing time/rpm): (1) 100/10/110, (2) 90/20/30, (3) 100/20/30, (4) 100/20/110, (5) 90/20/110, (6) 90/10/30, (7) 90/10/110, and (8) 100/10/30. The control was 95/15/70. [Color figure can be viewed in the online issue, which is available at www.interscience.wiley.com.]

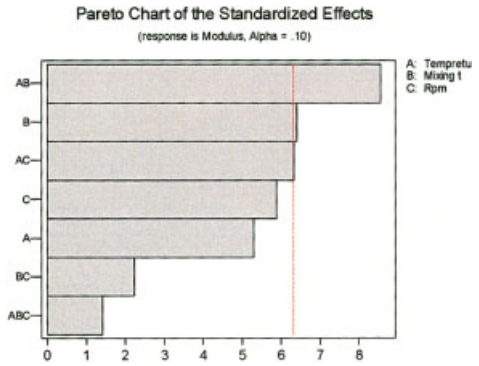

Figure 7 Pareto chart for the modulus. [Color figure can be viewed in the online issue, which is available at www.interscience.wiley.com.]

al.[13] This may be attributed to the intercalated particles acting as flaws in the polymer matrix. If a flaw exists within an area of stress concentration, the tensile strength and elongation will be reduced.[18]

The tensile modulus was taken as the response in the analysis of the experimental design, as it was the property showing the strongest dependence on the morphology. The Pareto chart and the normal probability plot of the standardized effects are shown in Figures 7 and 8. The Pareto chart is based on the analysis of variance. Here the null hypothesis that the individual factor effects and interactions between factors are equal is tested. In Figure 7, the dotted line shows the 90% confidence limit, and the bars crossing this line (i.e., AB, B, and AC) are the significant parameters at this confidence limit. The normal probability plot shows the relative nature of the effect of each significant parameter on the response. The straight line in Figure 8 is drawn under the assumption that none of the factors have a significant effect. The deviation from this line indicates the relative influence of that parameter on the response: the modulus. Because all the points deviate from this line, all the parameters have some effect on the response, but only labeled parameters are significant at the 90% confidence level.

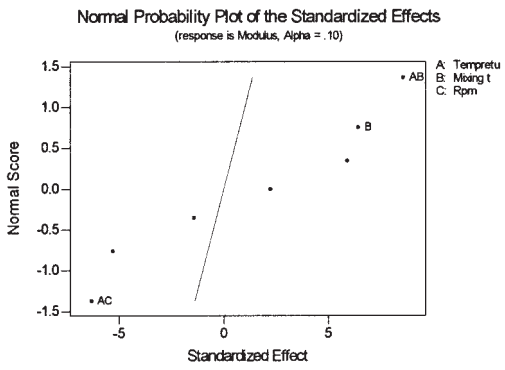

Figure 8 Normal probability plot of effects.

TABLE III
Coefficients of the Parameters in the Model of the Modulus

Term	Coefficient
Constant	−3811.44
Temperature (A)	87.39
Mixing time (B)	−30.15
rpm (C)	3.11
Temperature × Temperature (A^2)	−0.48
Temperature × Mixing time (AB)	0.33
Temperature × rpm (AC)	−0.03

Figure 8 shows that the interactions of the temperature and mixing time (AB) and the mixing time (B) have positive effects, whereas the interaction of the temperature and rotor speed (AC) has a negative effect, on the modulus. Figure 7 shows that the mixing time (B) is the only individual factor significant at the 90% confidence limit. This suggests that a longer time, lower temperature, and higher rotor speed (rpm) contribute most to a higher modulus and hence to the dispersion of clay into intercalated particles. These trends are consistent with the mechanism suggested by Dennis et al.,[9] in which a high shear intensity is required to start the dispersion process by breaking particles into tactoids and then a residence time in a low-shearing environment is required to allow the polymer to enter the clay galleries.

Response surface regression was used to find a relation between the parameters and the response. A linear model did not fit the response surface well. However, a second-order quadratic model fit well (R^2 = 97%). The coefficients of the parameters and interactions used in determining the model are given in Table III. The fitted model in general terms is given as follows:

$$Y = \beta_0 + \Sigma\beta_i x_i + \Sigma\beta_{ii} x_i^2 + \Sigma\Sigma\beta_{ij} x_i x_j$$

where β_0 is a constant; β_i is the coefficient of individual factors, β_{ii} is the coefficient of squared factors, β_{ij} is the coefficient of interactions, and x_n ($n = i$, j, or k) is a variable or factor.

The coefficients of the model obtained are given in Table III. The values represent the relative contributions of the parameters toward the response.

With the aforementioned model, contour plots were generated and are given in Figure 9. A contour is an equipotential curve in two dimensions on which the value of a function is constant. Therefore, it helps to identify the trends of the function with respect to two variables.

Both contour plots [Fig. 9(a,b)] are somewhat elongated. The nonlinearity of the plots reflects the complex pairwise interactions between the parameters. Factor interactions are as important as individual pa-

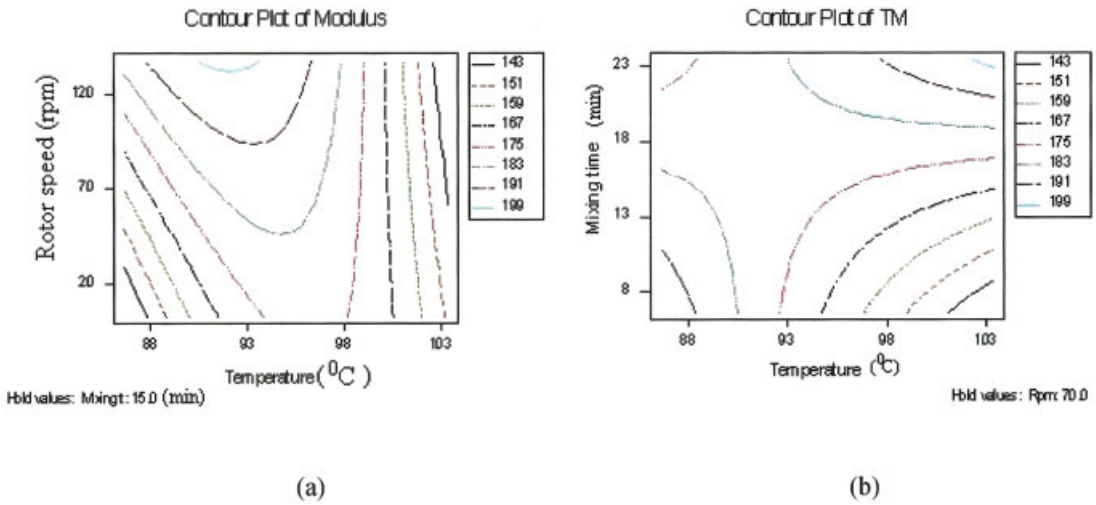

Figure 9 Contour plots of the tensile modulus (a) for the temperature versus the rotor speed and (b) for the temperature versus the mixing time. [Color figure can be viewed in the online issue, which is available at www.interscience.wiley.com.]

rameters in determining optimum processing conditions for the formation of nanocomposites. All functions show a point of maximum response, but this point is outside the experimental boundaries.

From the model, an optimum modulus for a mixing time of 15 min was predicted to occur around 90° C and 190 rpm (221 MPa). This point is beyond the boundaries of Figure 9(a) but is consistent with the general trends shown in the figure. An optimum modulus at 70 rpm was predicted to occur around 110°C and 35 min (225 MPa), as suggested by Figure 9(b). There could be several combinations of parameters that could produce similar properties.

Some of the optimum points predicted by the model were tested experimentally to check the accuracy of the model (Figs. 10 and 11). The experimental values agree well with the predicted values: most are within one standard deviation. In addition to higher modulus values, these samples also exhibited higher tensile strength and elongation at break, approaching the strength and elongation of the virgin polymer. This indicates that the filler particles were smaller and no longer acted as flaws in the polymer matrix. One sample (98/40/195) was as good as poly(ethylene vinyl acetate). Similar improvements in the tensile strength and elongation at break were reported by Joen et al.[13] for poly(ethylene vinyl acetate) (15% vinyl acetate)/organomodified clay composites with the addition of maleic anhydride grafted polyethylene.

The WAXS patterns of these nanocomposites are shown in Figure 12. The peak corresponding to d_{001} [$2\theta \sim 2°$ (44 Å)] is more prominent in Figure 12 than in Figure 2, and the second peak at $2\theta = 4.45°$ (19.8 Å) is somewhat smaller. The approximate peak positions are given in Table IV. The presence of two peaks confirms that the arrangement of clay is periodic, that is, intercalated. However, the full width at half-maximum (fwhm) of both the d_{001} and d_{002} peaks of WAXS patterns in Figure 12 is increased (broader peaks). The increased fwhm of both peaks and the loss of intensity of the d_{002} peak suggest a smaller particle size and disordered layer stacking.[19] Transmission electron microscopy images of these nanocomposites confirm these observations.[20] This suggests that even though these composites are an intercalated system (and not exfoliated), the number of platelets (layers) involved in a periodic arrangement is smaller in the composites produced under optimum mixing conditions. Hence, the clay is better distributed and dispersed, and the aspect ratio is higher; this exposes a greater surface

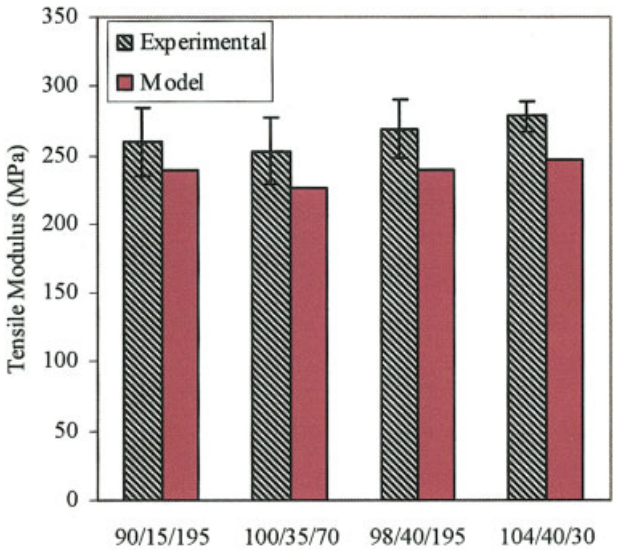

Figure 10 Tensile moduli of nanocomposites made at some optimum points predicted by the model. [Color figure can be viewed in the online issue, which is available at www.interscience.wiley.com.]

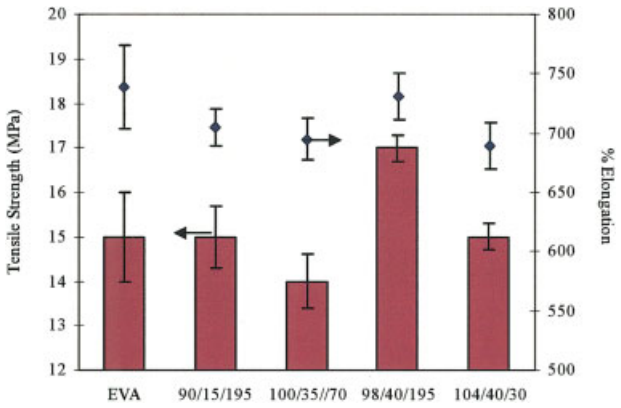

Figure 11 Tensile strength and elongation at break of nanocomposites made at some optimum points predicted by the model. The symbol ♦ refers to the elongation. [Color figure can be viewed in the online issue, which is available at www.interscience.wiley.com.]

area to the polymer matrix. This provides more efficient transfer of stress and hence improved modulus in these nanocomposites. These observations are consistent with the mechanical properties being superior for these composites. The smaller particles no longer act as flaws in the system, and the tensile strength and elongation at break are increased, becoming close or equal to those of the pure polymer.

CONCLUSIONS

EVA9 produced intercalated structures with organomodified sodium-type bentonite. A statistical experiment design was successfully used to optimize the processing conditions. Increasing the time and temperature increased the modulus significantly above

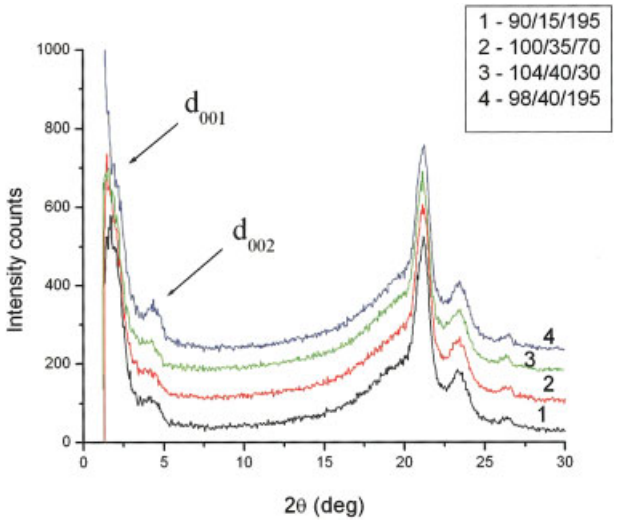

Figure 12 XRD patterns of cetyl nanocomposites made at optimum points. [Color figure can be viewed in the online issue, which is available at www.interscience.wiley.com.]

TABLE IV
Peak Data of Nanocomposites Made Under the Processing Conditions Predicted by the Model to be Optimum

Temperature/time/rpm	d_{001}		d_{002}	
	2θ (°)	Å	2θ (°)	Å
1-90/15/195	~1.9	46.02	~4.3	20.52
2-100/35/70	~1.8	49.02	~4.1	21.52
3-104/40/30	~1.8	49.02	~4.35	20.28
4-90/40/195	~2.05	43.04	~4.35	20.28

that of the polymer matrix. This was attributed to better dispersion and distribution of the intercalated clay. In addition to individual mixing parameters (temperature, mixing time, and rotor speed), their interactions also played a significant role in affecting the nanocomposite structure. Therefore, the interactions must be considered for successful optimization of the processing conditions. The tensile strength and elongation of the samples produced under optimized processing conditions were also improved and approached those of the polymer matrix.

References

1. Cater, L. W.; Hendricks, J. G.; Bolley, D. S. U.S. Pat. 2,531,396 (1958).
2. Usuki, A.; Kojima, Y.; Kawasumi, M.; Okada, A.; Fukushima, Y.; Kurauchi, T.; Kamigaito, O. J Mater Res 1993, 8, 1179.
3. Usuki, A.; Koiwai, A.; Kojima, Y.; Kawasumi, M.; Okada, A.; Kurauchi, T.; Kamigaito, O. J Appl Polym Sci 1995, 55, 119.
4. Okada, A.; Usuki, A. Mater Sci Eng C 1995, 3, 109.
5. Okada, A.; Fukushima, Y.; Kawasumi, M.; Inagaki, S.; Usuki, A.; Sugiyama, S.; Kurauchi, T.; Kamigaito, O. U.S. Pat. 4,739,007 (1988).
6. Giannelis, E. P.; Mehrotra, V.; Tse, O. K.; Vaia, R. A.; Sung, T. C. in Synthesis and Processing of Ceramics: Scientific Issues; Rhine, W. E.; Shaw, T. M.; Gottshall, R. J.; Chen, Y., Eds., MRS Proceedings: Pittsburgh, PA, 1992, 299, 547.
7. Vaia, R. A.; Giannelis, E. P. Macromolecules 1997, 30, 8000.
8. Vaia, R. A.; Ishii, H.; Giannelis, E. P. Chem Mater 1993, 5, 1694.
9. Dennis, H. R.; Hunter, D. L.; Chang, H.; Kim, S.; White, J. L.; Cho, J. W.; Paul, D. R. Polymer 2001, 42, 9513.
10. Mantia, F. P. L.; Verso, S. L.; Dintcheva, N. T. Macromol Mater Eng 2002, 287, 909.
11. Typical Physical Properties Bulletin, Closite 15A, 2001. www.nanoclay.com/data/15A.htm (Accessed April 2005).
12. Zannetti, M.; Camino, G.; Thomann, R.; Mulhaupt, R. Polymer 2001, 42, 4501.
13. Jeon, C. H.; Ryu, S. H.; Chang, Y.-W. Polym Int 2003, 52, 153.
14. Fornes, T. D.; Yoon, P. J.; Hunter, D. L.; Keskkula, H.; Paul, D. R. Polymer 2002, 43, 5915.
15. Alexandre, M.; Bayer, G.; Henrist, C.; Cloots, R.; Rulmont, A.; Jerome, R.; Dubois, P. Macromol Rapid Commun 2001, 22, 636.
16. Alexandre, M.; Beyer, G.; Henrist, C.; Cloots, R.; Rulmont, A.; Jerome, R.; Dubois, P. Chem Mater Commun 2001, 2, 4.
17. Alexandre, M.; Dubios, P. Mater Sci Eng 2000, 28, 1.
18. Griffith, A. A. Philos Trans R Soc London Ser A 1920, 221, 163.
19. Vaia, R. A. Materials Science and Engineering; Cornell University Press: Ithaca, NY, 1995; p 187.
20. Tillekeratne, M.; Jollands, M.; Cser, F.; Bhattacharya, S. No., to be submitted.